

Single-Crystal Field-Effect Transistors Based on Organic Selenium-Containing Semiconductor

To cite this article: Roswitha Zeis *et al* 2005 *Jpn. J. Appl. Phys.* **44** 3712

View the [article online](#) for updates and enhancements.

You may also like

- [Simple complex amplitude encoding of a phase-only hologram using binarized amplitude](#)
Tomoyoshi Shimobaba, Takayuki Takahashi, Yota Yamamoto et al.
- [Enhancement-mode field-effect transistors based on Ti-doped \$\text{In}_2\text{O}_3\$ nanowires fabricated by electrospinning](#)
Zhuodong Li, You Meng, Chao Wang et al.
- [Commercially available chromophores as low-cost efficient electron injection layers for organic light emitting diodes](#)
Apostolis Verykios, Anastasia Soultati, Konstantina Tourlouki et al.

Single-Crystal Field-Effect Transistors Based on Organic Selenium-Containing Semiconductor

Roswitha ZEIS, Christian KLOC, Kazuo TAKIMIYA¹, Yoshihito KUNUGI², Yasushi KONDA¹, Naoto NIIHARA¹ and Tetsuo OTSUBO¹

Bell Laboratories, Lucent Technologies, 600 Mountain Ave., Murray Hill, NJ 07974, U.S.A.

¹*Graduate School of Engineering, Hiroshima University, 1-4-1 Kagamiyama, Higashi-Hiroshima, Hiroshima 739-8527, Japan*

²*Faculty of Integrated Arts and Sciences, Hiroshima University, 1-7-1 Kagamiyama, Higashi-Hiroshima, Hiroshima 739-8521, Japan*

(Received November 10, 2004; accepted January 11, 2005; published June 10, 2005)

We report on the fabrication and characterization of single-crystal field-effect transistors (FETs) based on 2,6-diphenylbenzo[1,2-b:4,5-b']diselenophene (DPh-BDSe). These organic field-effect transistors (OFETs) function as p-channel accumulation-mode devices. At room temperature, for the best devices, the threshold voltage is less than -7 V and charge carrier mobility is nearly gate bias independent, ranging from 1 to $1.5 \text{ cm}^2/(\text{V s})$ depending on the source-drain bias. Mobility is increased slightly by cooling below room temperature and decreases below 280 K. [DOI: 10.1143/JJAP.44.3712]

KEYWORDS: organic semiconductor, field effect transistor, organic single crystal, mobility

1. Introduction

Organic semiconductors have received considerable attention within recent decades. Already the first “plastic electronic” products, such as displays that use organic light-emitting diodes, are on the market, setting the stage for organic semiconductor technology. This technology has potential applications for inexpensive printed devices like radio-frequency identification tags (RFIDs), low-end and high-volume data storage devices, flexible, cheap and therefore disposable displays and wearable computer devices. Organic solar cells and chemical sensors have recently attracted special attention.

For these above-mentioned applications, a better understanding of charge transport in organic semiconductor materials is required. Field-effect transistors (FETs) allow continuous tuning of charge density induced by the transverse electric field and enable the systematic study of charge carrier transport in organic materials. For our study, as a semiconductor, we chose 2,6-diphenylbenzo[1,2-b:4,5-b']diselenophene (DPh-BDSe), with the molecular structure shown in Fig. 1. The synthesis of DPh-BDSe has been reported recently.¹⁾

This material contains large selenium atoms which we hoped would improve the intermolecular interactions and allow efficient π electron transport between molecules, a concept which had already been demonstrated in thin-film field-effect transistors.¹⁾ Thin-film FETs were fabricated by an evaporation of organic semiconductors on the surface of strongly doped Si wafers with thermally grown SiO_2 layers. A relatively high mobility of $0.17 \text{ cm}^2/(\text{V s})$ and an on/off ratio larger than 10^5 had already been measured¹⁾ but we assumed that even better parameters might be obtained by avoiding grain boundaries, defects and limiting the concentration of impurities. Therefore, we use high-quality single crystals, graphite-painted electrodes and Parylene gate insulator for the fabrication of field effect transistors.

2. Experimental Details

The molecules were synthesized from commercially available *p*-dibromobenzene using a three-step reaction.¹⁾ For structure determination, single crystals were grown from

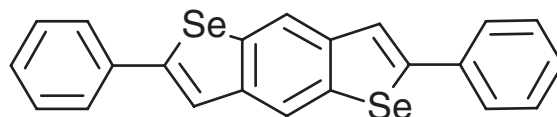


Fig. 1. Molecular structure of DPh-BDSe.

benzonitrile solution and a herringbone structure was determined using a Rigaku AFC7 single-crystal diffractometer. DPh-BDSe single crystals were grown by horizontal physical vapor transport in the flow of argon gas. Details of the growth technique have been reported elsewhere.²⁾ The evaporating material DPh-BDSe was heated to 300°C in the hot zone of a two-zone furnace. The second zone of the furnace was maintained at 200°C . We used two sublimations to purify the starting material. DPh-BDSe single crystals spontaneously grew on the wall of the glass tube in the colder zone of the furnace as pale yellow platelets with a surface area of up to $5 \times 5 \text{ mm}^2$ and a thickness of the order of $10 \mu\text{m}$. The structure of the gas-phase-grown DPh-BDSe single crystals was confirmed by X-ray diffraction analysis to be the same as that of the solvent-grown crystals.¹⁾

On the surface of the freshly grown crystals, a typical³⁾ field-effect transistor structure was produced (Fig. 2). Source

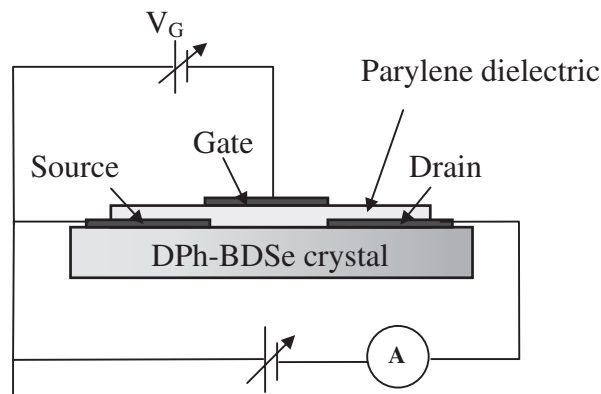


Fig. 2. Schematic representation of DPh-BDSe-based FET and measurement circuit.

and drain contacts were painted with a water-based solution of colloidal graphite. The gate-insulating layer consisted of a 1.1–1.7 μm -thick Parylene N thin film. The thickness of the films was determined with a profilometer. On top of the parylene layer, between the source and drain, the gate electrode was painted with the colloidal graphite. The channel capacitance was calculated from the thickness of the insulating layer and the tabulated dielectric constant of Parylene N. The transistor characteristics were measured at room temperature using a test fixture connected to a HP 4145B semiconductor parameter analyzer. The low-temperature measurements were performed in a helium atmosphere in a Quantum Design cryostat, which was also connected to a HP 4145B semiconductor parameter analyzer. To precisely control the temperature of the devices inside the Quantum Design cryostat, we used an additional temperature sensor placed near the sample.

During our work on the improvement of the transistor characteristics, we have noticed that such simple operations like evaporation of gold or silver contacts or sputtering of insulating oxides on the surface of single crystals may cause numerous defects. The presence of these defects, formed during FET fabrication, deteriorates the FET characteristics and FET mobilities. Therefore, we used here the gently painted electrodes and room-temperature deposited polymer, Parylene. These soft fabrication processes result in reproducible high mobility measured in numerous single-crystal FETs.

3. Results and Discussion

Figure 3 shows the source–drain current (I_{SD}) as a function of the applied source–drain voltage (V_{SD}) for different gate voltages (V_G). For small negative source–drain voltages (V_{SD}) the FET operates in the linear regime. When the source–drain voltage increases, the gate field is no longer uniform and a depletion area is formed at the drain contact. Beyond a certain source–drain voltage (V_{SD}), the current becomes saturated. This behavior is typical for a p-type field-effect transistor.

Plotted in Fig. 4 are the transconductance characteristics, for different source–drain voltages (V_{SD}). As these characteristics indicate, the DPh-BDSe single-crystal device does

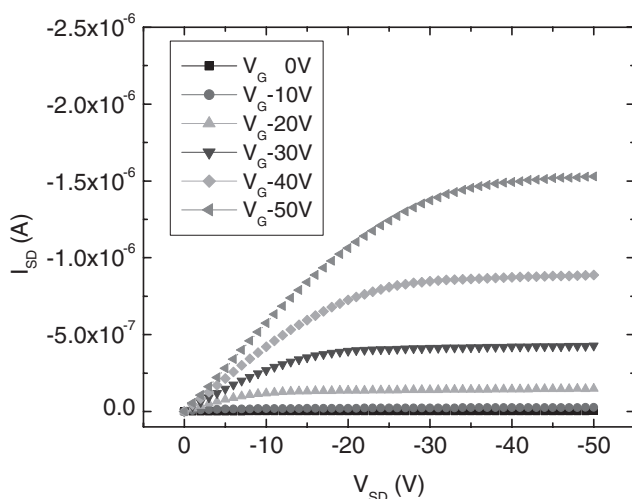


Fig. 3. Output characteristics of DPh-BDSe FET.

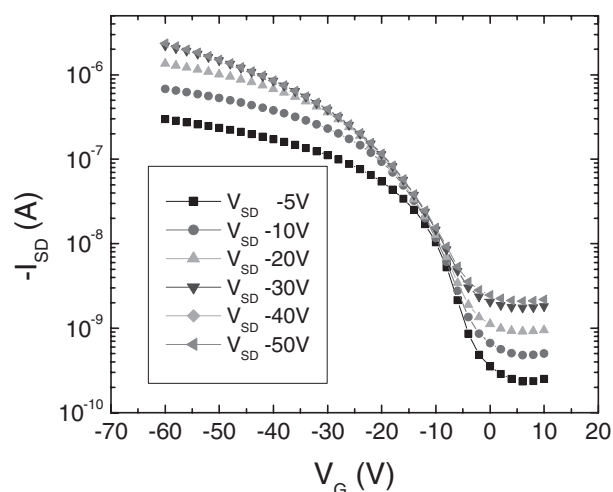


Fig. 4. Transconductance characteristics of DPh-BDSe FET (same device), for different source-drain voltages.

not develop a sharp field-effect onset. For small gate voltages, the source-drain current changes only gradually with the applied field. This feature might indicate the existence of a resistivity barrier on the contacts. The high contact resistance in a Schottky-type OFET depends nonlinearly on the gate voltages. A similar effect that dominates particularly in the subthreshold region has also been observed for rubrene single-crystal FETs.⁴⁾ However, the DPh-BDSe single-crystal devices exhibit, at $V_{SD} = -5$ V, a subthreshold swing (S) of approximately 7 V/decades, which corresponds to a normalized subthreshold swing (S_i) of $11 \text{ V} \cdot \text{nF}/\text{decade} \cdot \text{cm}^{-2}$. This value is comparable with a-Si:H FETs and CuPc single crystal FETs, for which $S_i = 10 \text{ V} \cdot \text{nF}/\text{decade} \cdot \text{cm}^{-2}$ ⁵⁾ and $S_i = 7 \text{ V} \cdot \text{nF}/\text{decade} \cdot \text{cm}^{-2}$ ⁶⁾ respectively have been reported. For comparison, in the best devices, rubrene single-crystal FETs, which usually develop a sharper field-effect onset, the normalised subthreshold swing is $S_i = 1.7 \text{ V} \cdot \text{nF}/\text{decade} \cdot \text{cm}^{-2}$.⁷⁾

The field-effect onset is observed at a negative gate voltage (-1 V). For a p-type device, this behavior resembles a “normally-off” FET, which seems to be the case for all organic single-crystal field-effect transistors with Parylene as a gate dielectric.^{6–8)} Assuming that the density of electrical active traps is proportional to the charge needed to fill these traps, and taking the threshold voltage of -7 V from Fig. 4, the density of the charged traps at the DPh-BDSe/Parylene interface is estimated to be $6.6 \times 10^{10} \text{ cm}^{-2}$. In this rough evaluation the contribution of the contacts on the threshold voltage has not been taken into account, but such a procedure allows us to estimate the upper limit of trap concentration.

Due to the relatively high bulk conductivity of this material, the on/off ratio of less than 10^4 was obtained from the transconductance characteristics. From the data presented in Fig. 4, we determined the charge carrier mobility in the linear regime ($V_{DS} > V_G - V_T$) by using the equation $\mu = (L/WC_i V_{SD})(dI_{SD}/dV_G)$,⁹⁾ where C_i is the gate insulator capacitance per unit area. As shown in Fig. 5, the field-effect mobility depends on the source-drain voltage. With increasing source–drain bias, the mobility increases until it saturates at $1.5 \text{ cm}^2/(\text{V} \cdot \text{s})$. This means that for a sufficiently large

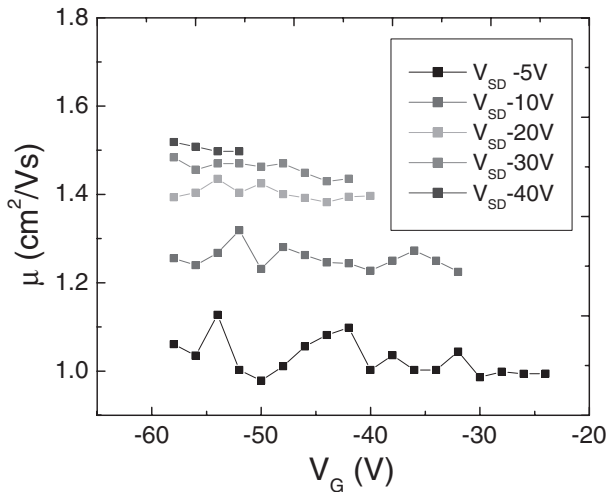


Fig. 5. Carrier mobility of DPh-BDSe FET in linear regime (obtained from data in Fig. 4).

longitudinal electric field the transistor performance is no longer limited due to the Schottky barrier of the contacts. If we calculate the mobility from the saturation regime ($V_{DS} > V_G - V_T$) applying the equation $\mu = 2(L/WC_i)(dI_{SD}/dV_G)^2$,⁹⁾ the equivalent behavior was found. In addition, we obtained the same maximum carrier mobility of $1.5 \text{ cm}^2/(\text{V s})$. Podzorov *et al.*⁷⁾ and Goldman *et al.*¹⁰⁾ have reported a similar source-drain bias dependence for rubrene single-crystal FETs. Figure 5 also indicates that for a sufficiently large negative gate bias ($V_G < -20 \text{ V}$) the carrier mobility becomes nearly independent of V_G . This feature reflects the high quality of the crystal, with only few structural defects.¹¹⁾

It is noteworthy that the mobility of $1.5 \text{ cm}^2/(\text{V s})$ is the highest value we obtain for our DPh-BDSe single-crystal devices, but mobilities above $1 \text{ cm}^2/(\text{V s})$ were routinely measured. Furthermore, compared with thin film devices, the mobility for single-crystal FETs is approximately one order of magnitude higher.¹⁾

Figure 6 shows a slight increase in carrier mobility with cooling until it reaches its maximum at 280 K. Below 280 K, the mobility drops rapidly and displays a thermally activated behavior. For a large number of trapping states present in the band gap, an Arrhenius-like dependence of the mobility $\mu \sim \exp(-E_A/k_b T)$ is to be expected. We determined an activation energy (E_A) of approximately 25 meV. However, we would like to add that, at low temperatures the Schottky barrier on the contacts may limit the source drain current and therefore the activation energy calculated from the two electrodes; the mobility may need to be corrected for this effect.

4. Conclusions

To increase the carrier mobility in aromatic compounds,

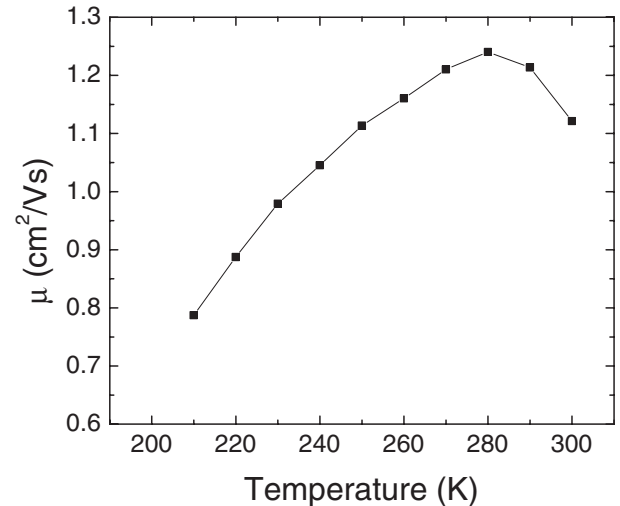


Fig. 6. Temperature dependence of carrier mobility calculated from square root of saturation current ($V_{SD} = -60 \text{ V}$).

we have introduced selenium atoms into the aromatic rings. We grew single crystals and prepared single-crystal FETs. We have found that a mobility as high as $1.5 \text{ cm}^2/(\text{V s})$ can be achieved and that mobility slightly increases with cooling following a strong decrease at low temperatures.

Acknowledgments

We thank Professor E. Bucher for his support and advice, W. So for fruitful discussions and C. G. MacLennan for reading the manuscript. R. Zeis acknowledges the financial support from the Konrad Adenauer Foundation, the German Academic Exchange Service (DAAD) and the Landesgraduiertenförderung Baden-Wuerttemberg. We acknowledge the support of the US Department of Energy under grant # 04SCPE389.

- 1) K. Takimiya, Y. Kunugi, Y. Konda, N. Niihara and T. Otsubo: *J. Am. Chem. Soc.* **126** (2004) 5084.
- 2) R. A. Laudise, C. Kloc, P. G. Simpkins and T. Siegrist: *J. Cryst. Growth* **187** (1998) 449.
- 3) V. Podzorov, V. M. Pudalov and M. E. Gershenson: *Appl. Phys. Lett.* **82** (2003) 1739.
- 4) R. W. I. D. Boer, M. E. Gershenson, A. F. Morpurgo and V. Podzorov: *Phys. Status Solidi A* **201** (2004) 1302.
- 5) J. Kanicki, F. R. Libsch, J. Griffith and R. Polastre: *J. Appl. Phys.* **69** (1991) 2339.
- 6) R. Zeis, T. Siegrist and C. Kloc: *Appl. Phys. Lett.* **86** (2005) 022103.
- 7) V. Podzorov, S. E. Sysoev, E. Loginova, V. M. Pudalov and M. E. Gershenson: *Appl. Phys. Lett.* **83** (2003) 3504.
- 8) V. Y. Butko, X. Chi and A. P. Ramirez: *Solid State Commun.* **128** (2003) 431.
- 9) S. M. Sze: *Semiconductor Devices: Physics and Technology* (Wiley, New York, 1985) 2nd ed.
- 10) C. Goldmann, S. Haas, C. Krellner, K. P. Pernstich, D. J. Grunlach and B. Batlogg: *J. Appl. Phys.* **96** (2004) 2080.
- 11) C. D. Dimitrakopoulos and P. R. L. Malenfant: *Adv. Mater.* **14** (2002) 99.